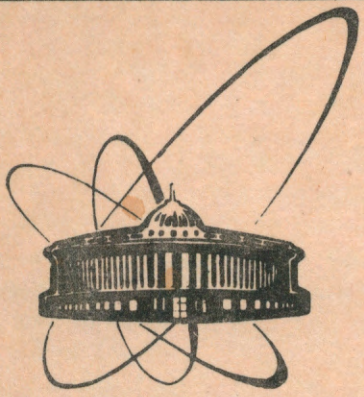

объединенный
институт
ядерных
исследований
дубна

E2-91-312

G.N.Afanasiev, V.M.Shilov

NUMERICAL INVESTIGATION OF TONOMURA EXPERIMENTS

Submitted to "Proc. Roy. Soc. London"

1991

I. Introduction

A recent discussion of the Aharonov - Bohm (AB) effect stems from the fact that multivalued wave-functions (wf) are admissible in multiconnected space regions. It turns out that literal use of multivalued wf (that is a solution of the Schroedinger equation in terms of multivalued wf) leads to the disappearance of the AB effect. It arises only if single-valued wf are used (see, e.g., [1,2]). The famous Pauli proof of wf's singlevaluedness holds only in simply connected space regions. Thus, this ambiguity should be resolved experimentally. The earlier experiments [3,4] in which electrons were scattered on the cylindrical solenoid are now generally considered as insufficient. The main reasons are bad asymptotics of wf (due to the long-range behaviour of the vector potential (vp)), the nonzero return flux and the magnetic field leakages (due to the finite length of the solenoid). This allows different physical interpretations of experimental data (see, e.g., lucid discussion in Berry's paper [5]). All these drawbacks are lacking for the toroidal solenoid (TS). The short-range behaviour of vp ($\sim r^{-3}$, see [6,7]) yields nondistorted asymptotics of wf. There is no return flux as the magnetic field is entirely inside TS. In the excellent experiments performed by the Japanese physicists (see their description in Peshkin and Tonomura's book [8]) the electron scattering on the impenetrable TS was studied. We shall refer to these experiments as Tonomura's experiments (TE). The shift of the diffraction pattern was observed there when the magnetic flux was switched on inside TS. Now we briefly review the existing theoretical approaches. In the important paper by Luboshitz and Smorodinsky [9] the electron diffraction on TS was considered in the framework of the Fraunhofer approximation. Unfortunately, this approximation fails due to the conditions under which TE were performed. The adequate approach was developed in refs. [10,11] . Based on this we aim here to give quantitative description of TE. The plan of our exposition is as follows. In § 2 the main computational formulae are presented and conditions for their validity are discussed. In § 3 the intensities of the scattered electrons are given for different values of the magnetic

flux inside TS and different positions of the registration plane. In § 4 the subtleties concerning TE are discussed and their comparison with theoretical intensities is presented. The short discussion of the results obtained is given in § 5. In what follows we shall always use singlevalued wf both in the presence or absence of magnetic fields, in simply or multiply connected space regions. After all, "The Aharonov - Bohm effect is real physics, not ideal physics" [12]. As far as we know the present treatment is the first one which quantitatively treats the AB effect for TS, thus making possible direct comparison with experimental data.

2. Technical Details

The following wf [10,11] describes the scattering of the plane electron wave exp (ikz) on the impenetrable TS

$$\psi = \exp(ikz) + \psi_s ,$$

$$\psi_s = i\,\frac{1+\cos\theta}{2}\cdot\exp(ikz)\cdot\exp\left(ik\,\frac{d^2+R^2}{2z}\right)\cdot \tag{2.1}$$

$$\cdot\left[\exp(i\omega)\cdot W_1 - \exp(2i\pi\gamma - i\omega)\cdot W_2\right].$$

Here d and R are the parameters of the impenetrable torus $(\rho-d)^2+z^2=R^2$ (fig.1) with the magnetic flux Φ inside it; θ and z are the scattering angle and distance from TS to the observation point P; $\omega = kdR/r$, W_1 and W_2 are the linear combinations of the Lommel functions of two variables

$$W_{1,2} = U_1\left[\frac{k\cdot(d\pm R)^2}{z}, k(d\pm R)\sin\theta\right] - i\,U_2\left[\frac{k(d\pm R)^2}{z}, k\cdot(d\pm R)\sin\theta\right].$$

The intensity is given by the absolute square of ψ : $I = |\psi|^2$. We discuss now conditions under which Eq. (2.1) is valid. It was obtained in the framework of the Fresnel - Kirchhoff (FK) diffraction theory [13,14]. It is suggested there that wf vanishes at the torus surface while outside the torus in the Z=0 plane it coincides with the plane wave (exp (ikz)). Then, at an arbitrary point P wf is given by the FK diffraction integral. It reduces to Eq.(2.1) if the following conditions are fulfilled:

$$k(d-R) \gg 1. \tag{2.2}$$

$$\delta\cdot\sin^2\theta \ll \pi \qquad (\delta = kd^2/2z). \tag{2.3}$$

In the experiment under consideration [15] $d \simeq 2\cdot10^{-4}$ cm, $R=10^{-4}$ cm, $K=2\cdot10^{10}$ cm^{-1} ($E \simeq 150$ keV). We shall study electron intensities in two z = const planes: z = 10 cm and z = 100 cm. To them there correspond values of δ equal to 4 and 0.4, resp. Then, Eq.(2.3) leads to the following restriction on $\sin\theta$: $\sin^2\theta \ll \pi/4$ for z =10 cm and $\sin^2\theta \ll 2\pi$ for z =100 cm. In TE the measurements were performed inside the solenoid's hole ($x \leq d-R$) and in the closest its vicinity. If we take $x_{max} = 2(d+R) \simeq 6\cdot10^{-4}$ cm, then $\sin\theta_{max}$ ($\simeq x_{max}/z$) equals $6\cdot10^{-5}$ for z =10 cm and $6\cdot10^{-6}$ for 100 cm. Thus inequality (2.3) is fulfilled. Now we discuss the validity of the FK boundary condition in TE. The special precautions were arranged in these experiments to prevent the particle penetration into the interior of TS (where $H \neq 0$). According to Tonomura [15] only 10^{-6} part of incident particles reaches this region. Thus impenetrability condition $\psi = 0$ on the torus surface is also satisfied. Further, approximation of wf by the plane wave in the part of the $z = 0$ plane lying outside the torus is justified if a large number of wavelengths is confined inside the torus hole. As in the treated case $K\cdot(d-R) \simeq 2\cdot10^6$, the FK boundary conditions are also satisfied. Numerical investigations [16] show that the FK diffraction theory works satisfactorily even if the wavelength is comparable with aperture dimensions. The condition (2.2) does not mean absence of diffraction phenomena. In fact, condition (2.3) defines the angular region where the Fresnel diffraction takes place. It is essential however that lateral extension of the electron beam should exceed the obstacle dimensions. This fact has recently been admitted by Matteucci [17] who presented the excellent diffraction patterns for which the ratio of scatterer dimensions to the electron wavelength was of the order 10^3 - 10^4 .

3. Theoretical Analysis of Electron Diffraction by Toroidal Solenoid

In figs.2-5 there are shown typical electron intensities in the z =const plane. It turns out that inspite of its aesthetic form, Eq.(2.1) is inconvenient for practical computations. The FK diffraction integral was evaluated by using the method suggested by Burch /18/. The error of this method is approximately 3%. The parameters R, d and k are the same as in TE: $R=10^{-4}$ cm, $d=2\cdot10^{-4}$ cm, $K=2.10^{10}$ cm^{-1} (this corresponds to the electron energy $E \approx 150$ KeV). The values of $\gamma (=e\Phi/hc)$ are taken to be 0 and 1/2. This does not mean the loss of generality as the theory is invariant under the shift $\gamma \to \gamma+n$ (n is an integer). Consider first the case when the distance z from the $z=0$ plane to the registration one is chosen to be 10 cm (figs.2 and 3). We observe a small value of the electron intensity in the shadow region ($1 < x < 3$). For greater distances from the z axis electron intensities are practically the same for $\gamma = 0$ and $\gamma = 1/2$. They oscillate around the value $|\psi|^2 = 1$. The amplitude of oscillations damps as x grows. For x lying inside the torus hole ($x < 1$) the intensities for $\gamma = 0$ and $\gamma = 1/2$ differ appreciably (fig.4). Most of the oscillations are in a counterphase there. In fig.5 the same intensities are presented in the $z = 100$ cm plane. Only one oscillation is observed inside the torus hole. The shadow region is not so strongly pronounced as in the previous case (as it should be). In fig.6 there are shown intensities along the z axis. For this case Eq.(2.1) is considerably simplified, and we have

$$|\psi|^2 = 1 - 8\cdot\sin\left[\frac{K\cdot(d-R)^2}{4z}\right]\cdot\sin\left(\frac{KdR}{z}-\pi\gamma\right)\cdot$$

$$\cdot\cos\left[\frac{K(d+R)^2}{4z}-\pi\gamma\right].$$

We see that maxima of $|\psi|^2$ along the symmetry axis are macroscopically separated for $\gamma = 0$ and $\gamma = 1/2$. It is unclear however how to realize this measurement in practice. In fact, small value of the torus hole (2 μm in diameter) and the finiteness of the detector dimensions will necessarily lead to the averaging of intensities. Due to the conservation of the particle flux these integrated intensities will be practically the same and they hardly could be resolved experimentally.

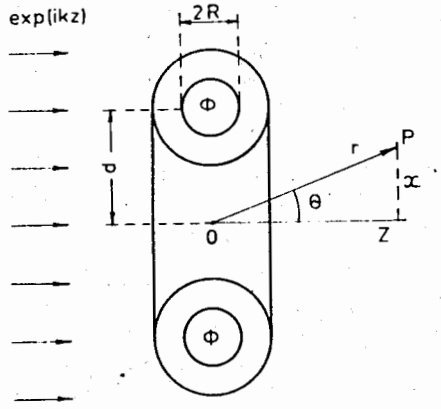

Fig.1. The schematic presentation of charged particles scattering on the impenetrable TS with the magnetic flux Φ inside it. R and d are the parameters of TS, z and x are the position of the registration plane and the distance of the observation point from the symmetry axis of TS.

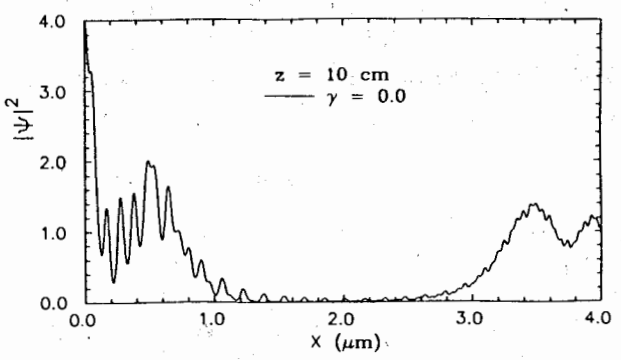

Fig.2. The intensity of scattered electrons in the Z=0 cm plane for the zero magnetic flux ($\gamma = e\Phi/hc = 0$). The intervals $0 < x < 1$ and $1 < x < 3$ correspond to the torus hole and the shadow region, resp.

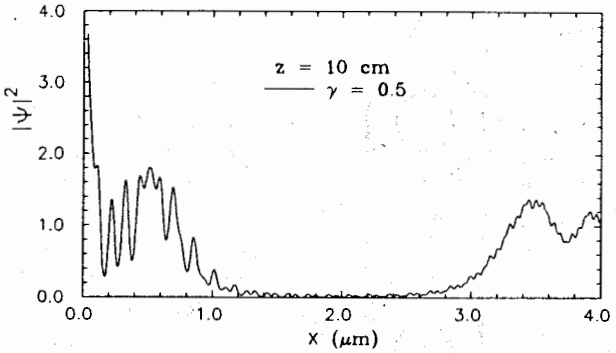

Fig.3. The same as in fig.2 but for $\gamma = 1/2$.

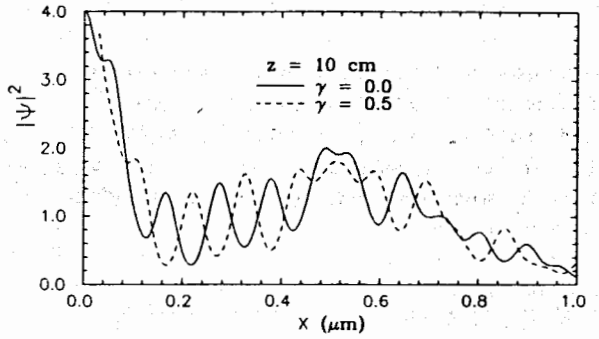

Fig.4. The intensities of two previous figs. are shown inside the hole of TS.

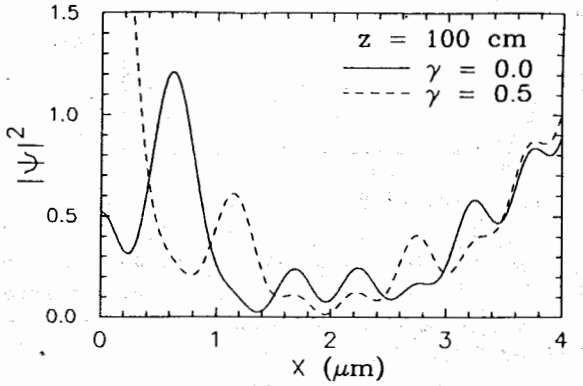

Fig.5. The intensities of scattered electrons in the Z=100 cm plane.

4. Tonomura Experiments

In the preceding section we have considered the diffraction of a plane electron wave on the impenetrable TS. However, TE were performed in a slightly different form (fig.7). An incoming electron beam is splitted in two parts. The first of them illuminates TS. The second part of the beam (which is referred to as a reference wave) is directed to the first part by using electron optical system and they both meet behind the TS. As a result, the interference pattern arises there. The experiment shows that in the space region II (where ψ_{ref} interferences with the part (ψ_{out}) of the beam which has not passed the torus hole) the interference picture remains the same for any value of the magnetic flux Φ . In the region I (where ψ_{ref} interferes with the part ψ_{in} of the beam which has passed the torus hole) the interference picture shifts with changing Φ .

Qualitative consideration . The usual explanation proceeds along the following lines. Let us suggest that in the absence of the magnetic field the wf ψ_{in} and ψ_{out} may be well approximated by the plane waves: $\psi_{in} = \psi_{out} = \exp(ikz)$. Further, let the wave vector of the reference wave have the components $k_x = k \cdot \sin\alpha$ and $k_z = k\cos\alpha$. Then $\psi_{ref} = \exp[ik(x\sin\alpha + z\cos\alpha)]$. In the absence of the magnetic field, we have in I and II: ψ_0 = $= \exp(ikz) + \psi_{ref}$ and $|\psi_0|^2 = 2\cdot\{1+\cos[kx\sin\alpha - kz\cdot(1-\cos\alpha)]\}$. In the plane z =const (where the measurements are performed) the maxima of $|\psi_0|^2$ are situated at $x_n^0 = [2\pi n + kz\cdot(1-\cos\alpha)]/k\sin\alpha$. The difference between them is Δx_n^0 = $= 2\pi/k\sin\alpha$. The presence of the magnetic field may be taken into account by the Dirac phase factor (see, e.g. [19]): $\psi_{in}^{\Phi} = \psi_{out}^{\Phi} = \exp(ikz)\exp\left(\frac{ie}{\hbar c}\int_{-\infty}^{z} A_z(x,z)\,dz\right)$. Here A_z is vp of TS. In spite of the same functional form this factor is different for ψ_{in}^{Φ} and ψ_{out}^{Φ} due to different values of x (see fig.1). Due to a short-range behaviour of A_z (at large distances $A_z \sim z^{-3}$, see [6,7]) the upper integration limit may be changed to $+\infty$. As $\int_{-\infty}^{\infty} A_z\,dz$ equals Φ if the integration axis passes through the solenoid's hole and zero otherwise, then ψ_{out} = $= \exp(ikz)$ and ψ_{in} = $\exp(ikz)\cdot\exp(2i\pi\gamma)$. This means that in the space region II the interference picture remains the same as in the absence of the magnetic field while in I $|\psi_I^{\Phi}|^2 = 2\cdot\{1+\cos[kx\sin\alpha - kz\cdot(1-\cos\alpha) - 2\pi\gamma]\}$. The maxima of $|\psi_I^{\Phi}|^2$ are at $x_n^{\Phi} = x_n^0 + 2\pi\gamma/k\sin\alpha$; that is the

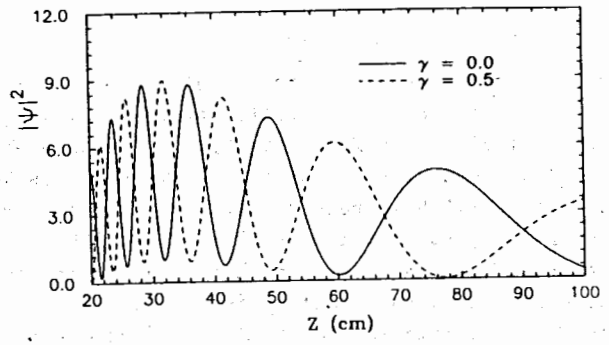

Fig.6. The electron intensities at the Z axis.

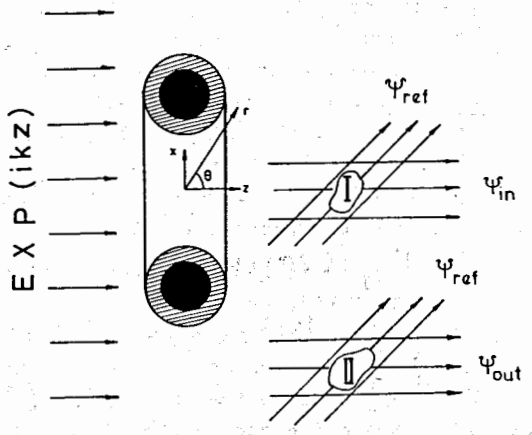

Fig.7. The schematic presentation of Tonomura experiments.

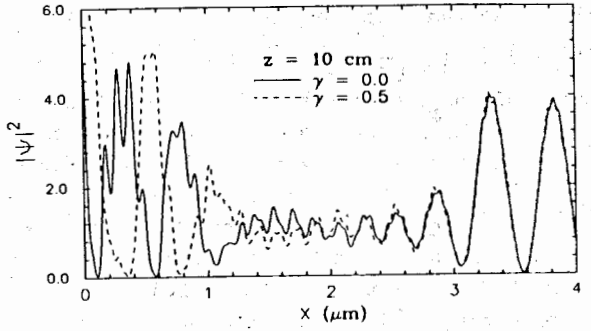

Fig.8. The intensities corresponding to the superposition of the scattered and reference electron waves in the Z=10 cm plane. The incidence angle of the reference wave is $\alpha \simeq 2\pi \cdot 10^{-6}$ rad.

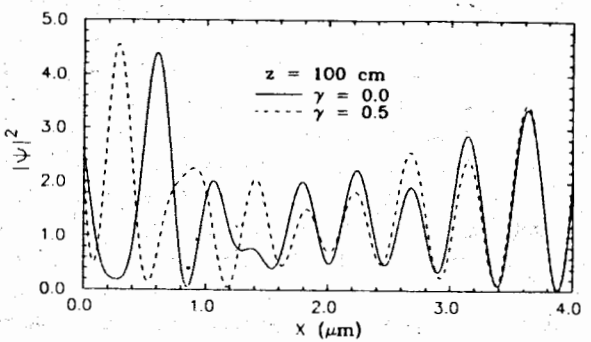

Fig.9. The same as in Fig.8 but for Z=100 cm.

switching on of the magnetic field shifts them onto $\Delta = 2\pi\gamma/\kappa\sin\alpha$. Due to the periodicity of $|\psi_i^{\Phi}|^2$ wrt γ it follows that it is enough to consider $0 < \gamma < 1$. Thus, the largest difference of the interference picture takes place for $\gamma = 1/2 : \Delta = \pi/\kappa\sin\alpha$.

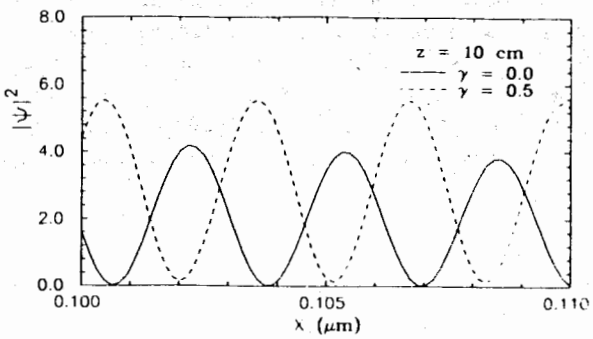

Fig.10. The same as in Fig.8 but for the incidence angle $\alpha = 10^{-3}$ rad. Only part of the interference picture ($0.1\ \mu m \leq x < 0.11\ \mu m$) is shown.

Quantitative consideration. To obtain quantitative results we superpose wf ψ given by Eq.(2.1) with ψ_{ref}. The results of calculations are presented in figs.8,9. The incidence angle α is chosen to be $2\pi \cdot 10^{-6}$ rad. We observe that maxima of $|\psi_t \psi_{ref}|^2$ are enough separated inside the torus hole. The intensities oscillate around the value 1 inside the shadow region (where $|\psi|$ is small and $|\psi_{ref}| = 1$) and around the value 2 outside the hole ($\chi > 3$) (as both ψ and ψ_{ref} are of the same order ($\simeq 1$)) but with different phases). In the paper by Tonomura et al. [15] the incidence angle α was estimated to be 10^{-3} rad. For this α and Z=100cm the computed interference picture is presented in fig.10. Notice the scale on the horizontal axis: the shown interference picture is displayed at the distance $10^{-2}\mu m$. From this fig. we estimate the distance between the successive maxima $\approx 3.2 \cdot 10^{-3}\mu m$ while the shift of the interference picture (due to the magnetic field switching on) equals approximately half of this value (for $\gamma = 1/2$). This agrees with qualitative estimates given above ($\Delta\chi_n^0 \approx 3.14\ 10^{-3}\mu m$, $\Delta \simeq 1.57\ 10^{-3}\mu m$). This interference picture is recorded on photofilm. Then, using a holography method the original diffraction picture (that is diffraction picture in the absence of a reference wave) is reconstructed. From the figures presented in the paper by Tonomura et al. [15] we estimate the distance between the neighbouring maxima $\approx 0.5\mu m$, while the shift of the particular maximum arising from the magnetic field switching on is $\Delta \simeq 0.25\mu m$ (for $\gamma = 1/2$). To compare with theory, one should know the distance z between TS and observation plane. We did not find any information concerning this distance in all available publications [8,15,20-22] treating this subject. From figs. 4-6 we find the diffraction pattern shift $\Delta \simeq 0.06\mu m$ for Z=100 cm and $\Delta \simeq 0.4\mu m$ for Z=100 cm. Thus, the observation plane in TE should lie between these values of z.

5. Conclusion

Three points should be mentioned at the end. First, the diffraction picture observed in TE is a superposition of particular electron events. Under this we mean the scattering of a particular electron on the impenetrable TS and its subsequent collapse at the registration screen. In fact, the intensity of the emitted electrons in TE

was so low that only one electron was inside the experimental installation at one particular instant of time [8,23]. Second, the adequacy of the FK diffraction theory for the description of electron scattering is supported by the thorough analysis of theoretical and experimental diffraction patterns (see, e.g., [14]). Third, the recent communication (Fink et al. [24]) on the use of coherent point sources of low-energy ($\sim$20-50 eV) electrons should be mentioned. According to these authors' claim the magnification up to 150000 times (comparing with that for the plane incoming wave) may be obtained for small distances between the electron emitter and the object under investigation. This opens new possibilities for studying enclosed field effects.

References

1. Aharonov Y., 1984, In: Proc.Int.Symp.Foundations of Quantum Mechanics (ed. S.Kamefuchi) pp.10-19, Tokyo: Japan Physical Society.
2. Yang C.N., 1984, In: Proc. Int.Symp.Foundations of Quantum Mechanics (ed.S.Kamefuchi), pp.5-9, Tokyo: Japan Phys.Soc.
3. Chambers R.G., 1960, Phys.Rev.Lett., 5, 3-5.
4. Mollenstedt G. and Bayh W., 1962, Naturwiss., 49, 81-82.
5. Berry M.V., 1980, Eur.J.Phys., 1, 154-162.
6. Afanasiev G.N., 1987, J.Comput.Phys. 69, 196-208.
7. Afanasiev G.N., 1990, J.Phys.A 23, 5755-5764.
8. Peshkin M. and Tonomura A., 1989, The Aharonov - Bohm Effect. Berlin e.a.: Springer.
9. Luboshitz V.L. and Smorodinsky J.A., 1978, Zh.Eksp.Teor.Fiz., 75, 40-46.
10. Afanasiev G.N., 1989, Phys.Lett. A142, 222-226.
11. Afanasiev G.N. and Shilov V.M., 1989, J.Phys.A 22, 5195-5216.
12. Berry M.V., 1986, In: Fundamental Aspects of Quantum Theory (eds. V.Gorini and A.Frigerio). Nato ASI Series vol.144, pp.319-320. New York: Plenum.
13. Born M. and Wolf E., 1980, Principles of Optics, 6th ed., Oxford, Pergamon.
14. Komrska J., 1971, In: Adv.in Electronics and Electron Physics, vol. 30, pp.139-234.
15. Tonomura A., Osakabe N., Matsuda T., Kawasaki T., Yano S., Yamada H., 1986, Phys.Rev. A34, 815-822.
16. Silver S., 1962, J.Opt.Soc.Amer., 52, 131-139.

17. Matteucci G., 1990, Amer.J.Phys., 58, 1143-1147.
18. Burch D.S., 1985, Amer.J.Phys., 53, 255-260.
19. Berry M.V., 1980, Eur.J.Phys., 2, 240-244.
20. Tonomura A., Yano S., Osakabe N., Matsuda T., Yamada H., Kawasaki T., Endo J., 1987, In: Proc. 2nd Int.Symp.Foundations of Quantum Mechanics (eds.: M.Namiki, Y.Ohnuki, Y.Murayama, S.Nomura) pp.97-105, Tokyo: Japan Phys. Soc.
21. Tonomura A., 1988, Physica B151, p.206-213.
22. Tonomura A., 1989, Int.J.Mod.Phys. B3, p.521-533.
23. Tonomura A., Endo J., Matsuda T., Kawasaki T., 1989, Amer.J.Phys., 58, p.117-120.
24. Fink H.W., Stocker W., Schmid H., 1990, Phys.Rev.Lett., 65, p.1204-1206.

Received by Publishing Department
on July 5, 1991.

Афанасьев Г.Н., Шилов В.М. E2-91-312

Численный анализ экспериментов Тономуры

Дан численный анализ экспериментов Тономуры по проверке существования эффекта Аронова - Бома. Интенсивность рассеянных электронов получена для различных значений магнитного потока внутри соленоида и различных положений плоскости измерения.

Работа выполнена в Лаборатории теоретической физики ОИЯИ.

Препринт Объединенного института ядерных исследований. Дубна 1991

Afanasiev G.N., Shilov V.M. E2-91-312

Numerical Investigation of Tonomura Experiments

The quantitative theoretical analysis of Tonomura experiments testing the existence of the Aharonov - Bohm effect is given. The intensities of scattered electrons are computed for different values of the magnetic flux and positions of the observation plane.

The investigation has been performed at the Laboratory of Theoretical Physics, JINR.

Preprint of the Joint Institute for Nuclear Research. Dubna 1991